



Geophysical Research Letters°

RESEARCH LETTER

10.1029/2024GL110078

Key Points:

- From a 2005–2006 simulation, it takes about 3 years for water to reach the grounding lines from the edge of the Amundsen Sea Embayment
- The simulation shows the Antarctic Coastal Current contributing equal amounts of water to Pine Island and Thwaites as off-shelf sources
- SOhi results indicate that 1/4 to 2/3 of the cooling between the shelf break and the grounding lines occurs within the cavities

Supporting Information:

Supporting Information may be found in the online version of this article.

Correspondence to:

A. Dinh, andy.dinh@uci.edu

Citation:

Dinh, A., Rignot, E., Mazloff, M., & Fenty, I. (2024). Modeling ocean heat transport to the grounding lines of Pine Island, Thwaites, Smith, and Kohler glaciers, West Antarctica. *Geophysical Research Letters*, 51, e2024GL110078. https://doi.org/10.1029/2024GL110078

Received 7 MAY 2024 Accepted 13 SEP 2024

© 2024. The Author(s). Geophysical Research Letters published by Wiley Periodicals LLC on behalf of American Geophysical Union.

This is an open access article under the terms of the Creative Commons Attribution License, which permits use, distribution and reproduction in any medium, provided the original work is properly cited.

Modeling Ocean Heat Transport to the Grounding Lines of Pine Island, Thwaites, Smith, and Kohler Glaciers, West Antarctica

Andy Dinh¹, Eric Rignot^{1,2,3}, Matthew Mazloff⁴, and Ian Fenty³

¹Department Earth System Science, University of California Irvine, Irvine, CA, USA, ²Department Civil and Environmental Engineering, University of California Irvine, Irvine, CA, USA, ³Jet Propulsion Laboratory, California Institute of Technology, Pasadena, CA, USA, ⁴Scripps Institution of Oceanography, University of California San Diego, Irvine, CA, USA

Abstract Pine Island, Thwaites, Smith, and Kohler glaciers in the Amundsen Sea Embayment (ASE) sector of West Antarctica experience rapid mass loss and grounding line retreat due to enhanced ocean thermal forcing from Circumpolar Deep Water (CDW) reaching the grounding lines. We use simulated Lagrangian particles advected with a looping 1 year output from the Southern Ocean high-resolution model to backtrack the transport and cooling of CDW to these glaciers. For the simulated year 2005–2006, we find that the median time needed to reach the grounding lines from the edge of the ASE is 3 years. In addition, the Antarctic Coastal Current contributes an equal number of particles as off-shelf sources to the grounding lines of Pine Island and Thwaites. For CDW coming from off-shelf, results from SOhi indicate that 25%–66% of the cooling occurs within ice shelf cavities.

Plain Language Summary The glaciers in the Amundsen Sea Embayment (ASE) sector of West Antarctica are contributing rapidly to sea level rise in response to enhanced melt by warm, salty Circumpolar Deep Water (CDW). We use an ocean numerical model to trace the sources, pathways, and cooling of warm waters to reach glacier grounding lines. We find that it takes multiple years for off-shelf perturbations to reach the glaciers and that the colder Antarctic Coastal Current contributes the same amount of water to the grounding lines of Thwaites and Pine Island glaciers as off-shelf CDW sources. The model also reveals that half of the cooling of CDW occurs under the ice shelves, which is an effect not accounted for in most models used for projecting sea level rise.

1. Introduction

The glaciers in the Amundsen Sea Embayment (ASE) of West Antarctica are a significant source of sea level rise (Rignot et al., 2019) due to changes in glacier dynamics (Rignot et al., 2008; Velicogna et al., 2014). A major driver is basal melting caused by the intrusions of warm, salty Circumpolar Deep Water (CDW) onto the continental shelf (Dinniman et al., 2012; Dotto et al., 2019; Wåhlin et al., 2012). The loss of basal ice reduces buttressing, allows the glaciers to accelerate, and contributes to sea level rise (Gudmundsson et al., 2019; Pritchard et al., 2012). For glaciers resting on a bed with a retrograde slope, that is, bed elevation decreases in the inland direction, enhanced basal melting of ice may lead to a positive feedback loop that triggers an irreversible retreat of the grounding line (Joughin et al., 2014; Rignot et al., 2014; Weertman, 1974).

The ASE is particularly sensitive to ocean thermal forcing because it has a weak slope current and lacks a strong density gradient to prevent CDW from flooding the continental shelf (Thompson et al., 2018). In recent decades, studies suggest that anthropogenic forcing may have played a role in strengthening the eastward flowing undercurrent, transporting additional CDW onto the continental shelf through a number of submarine troughs on the seafloor (Holland et al., 2022; Naughten et al., 2022). CDW mixes with on-shelf water to produce modified CDW that flows into ice shelf cavities and melts glacier ice at the grounding lines (Dutrieux et al., 2014; Nakayama et al., 2018). Pine Island, Thwaites, Smith, and Kohler glaciers experience rapid ice shelf melt (Adusumilli et al., 2020; Rignot et al., 2013) and grounding line retreat (Rignot et al., 2014). Understanding the transport of CDW to the grounding lines is crucial to improving the accuracy of ice-sheet/ocean models and sea level rise projections in the coming decades (Nowicki & Seroussi, 2018).

DINH ET AL.

Here, we use 1 year of output products (Sep 2005–Aug 2006) from the Southern Ocean high-resolution model (SOhi) and simulated Lagrangian particles to study the transport and cooling of CDW to the grounding lines of Pine Island, Thwaites, Smith, and Kohler glaciers. To the best of our knowledge, this is the first study that backtraces CDW at the grounding lines of these four glaciers to quantify the contributions from various CDW sources, the pathways on the continental shelf, and the timescale and magnitude of cooling during transport.

2. Data and Methods

2.1. Southern Ocean Model

We use 1 year (1 September 2005 to 31 August 2006) of 6-hourly average outputs from the Southern Ocean high-resolution (SOhi) simulation (Dinh et al., 2024b). SOhi is a 1/24° pan-antarctic simulation with 225 vertical levels that includes sea ice, oceanic tides, and all ice shelves. Bathymetry is from the General Bathymetric Chart of the Oceans 2020 (GEBCO Bathymetric Compilation Group, 2020, 2020) and ice cavity geometry is from Bed-Machine v1.39 (Morlighem, 2019). With a horizontal resolution of 1 km at 75°S, SOhi resolves eddy processes responsible for the transport of heat onto and across the continental shelf (St-Laurent et al., 2013; Stewart & Thompson, 2015). In addition, 225 vertical levels (z-spacing of 1.4 m at the surface, 25.8 m at 1,000 m, and 50 m at 3,000 m) allows SOhi to resolve processes within thin water columns inside ice shelf cavities.

We evaluate SOhi by comparing the speed of ocean currents with mooring data between 630 and 730 m depth near Pine Island. We find that SOhi currents are slightly slower by $0.5-2 \,\mathrm{cm}\,\mathrm{s}^{-1}$, but the error is within the observed range of variability (Figure S1 in Supporting Information S1). We also compare the mean temperature and salinity from SOhi to measurements taken from two cruises in 2008 and 2009. Overall, SOhi captures the major water masses in this region (Figure S2 in Supporting Information S1) except for the warmest and freshest waters. These less-well-represented waters are summer surface waters with properties that are likely averaged out in the SOhi yearly means. Structurally, as noted in Dinh et al. (2024b), the pycnocline in SOhi is similar to that in the Southern Ocean State Estimate (Mazloff et al., 2010) and Estimating the Circulation and Climate of the Ocean version 4 release 4 (ECCO Consortium et al., 2021), but 200 m too shallow compared to in-situ measurements. For temperature and salinity, the largest differences occur between 200 and 400 m due to the mismatched thermocline (Figure S3 in Supporting Information S1). At deeper depths, the mCDW in SOhi is about 0.5 C warmer and 0.1 psu saltier than observations (Dinh et al., 2024b).

We crop the SOhi outputs to a domain covering the ASE and the Bellingshausen Sea $(140^{\circ}\text{W} \text{ to } 65^{\circ}\text{W} \text{ and } 69^{\circ}\text{S} \text{ to } 75.5^{\circ}\text{S})$ (Figure 1a). We define the ASE region as the sector south of the 700 m isobath between 136°W and 98°W . The continental shelf West of 136°W is referred to as "west-shelf". The continental shelf East of 97°W is referred to as "east-shelf". Everything north of the 700 m isobath is "off-shelf" waters. Waters in the ASE are referred to as "on-shelf". Additionally, we split the off-shelf boundary between 122°W and 97°W into 4 sections corresponding to 4 submarine troughs: (a) Dotson-Getz Trough (DGT; $122^{\circ}\text{W} - 115^{\circ}\text{W}$), (b) Pine Island Trough West (PITW; $115^{\circ}\text{W} - 110^{\circ}\text{W}$), (c) Pine Island Trough East (PITE; $110^{\circ}\text{W} - 104^{\circ}\text{W}$), and (d) Abbot Trough (AT; $104^{\circ}\text{W} - 97^{\circ}\text{W}$).

2.2. Lagrangian Particles

Lagrangian particle trajectories have been previously used to investigate the pathways of CDW to the grounding lines of glaciers (Nakayama et al., 2019) and connectivity around Antarctica (Dawson et al., 2023). Here, we use particles to represent CDW at the grounding lines and trace them backwards in time to identify the sources, pathways, and changes in temperature of the water parcels. We consider the area in front of the grounding lines where the bed is deeper than 1,000 m to be "near the grounding lines" (Figures 1b–1d) and assume that water there will melt ice at the grounding line. We seed 1,000 particles near the grounding lines of each glacier. The particles are placed at the center of each horizontal grid cell (~l-km apart) and equally spaced in the vertical, covering the first 100 m from the sea floor. We release the particles daily for 1 year for a total 360,000 to 400,000 particles per glacier.

We run the Lagrangian tracers simulation offline using OceanParcels v2.4.1 (Delandmeter & Van Sebille, 2019) and 6-hourly outputs from SOhi. The particle are advected backward in time for 3 year using a fourth-order Runge-Kutta method with looping velocity fields. Although looping the field leads to a discontinuous jump in particle velocities, this step is necessary due to the finite duration of SOhi has been used in previous studies

DINH ET AL. 2 of 11

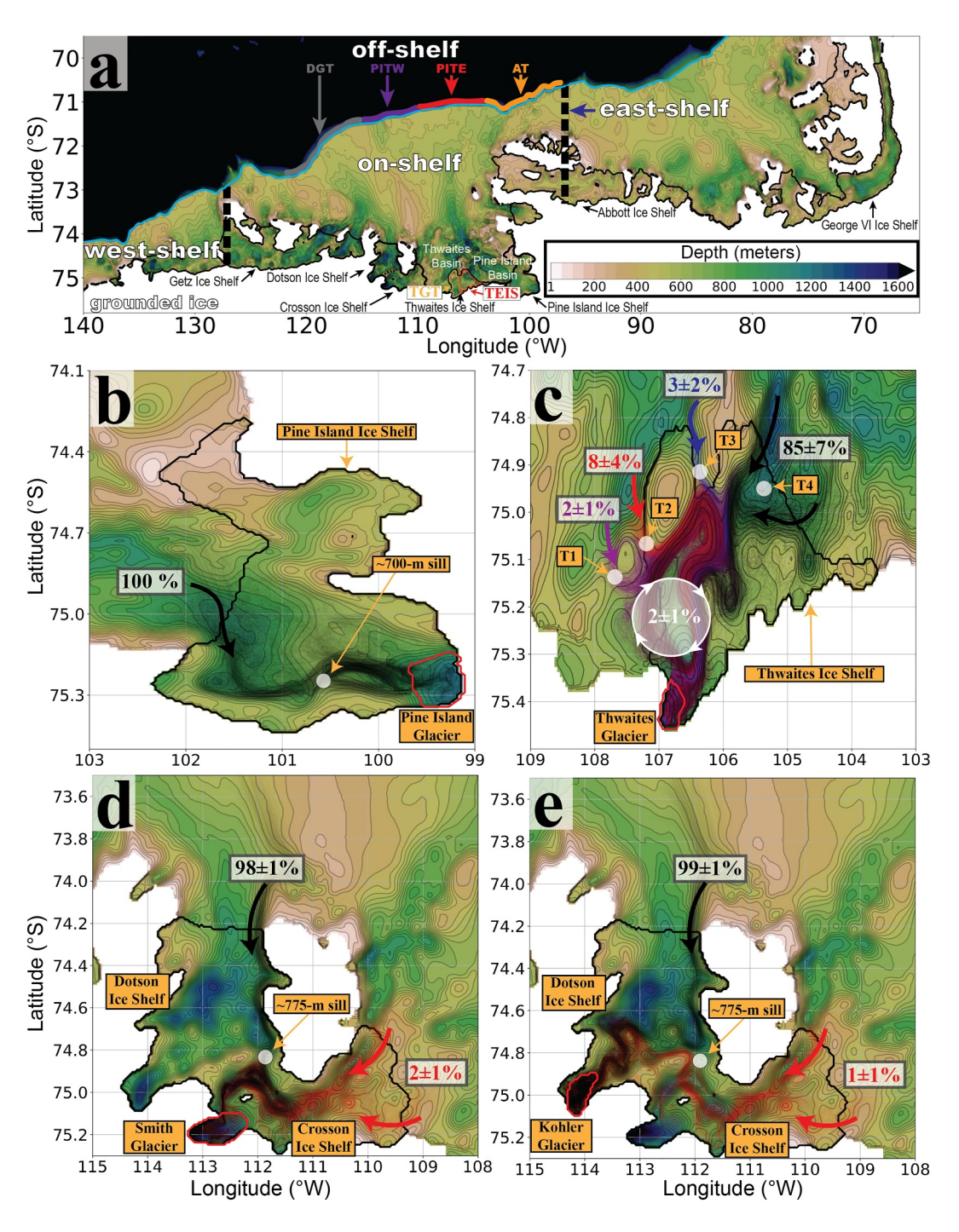


Figure 1. Map of the study area showing (a) an overview with on-shelf, east-shelf, west-shelf, and off-shelf boundaries in black overlaid on the bathymetry. The 700 m isobath between the on-shelf and off-shelf is in cyan. Labels indicate the Dotson-Getz Trough (DGT), Pine Island Trough West (PITW), Pine Island Trough East (PITE), Abbot Trough (AT), Thwaites Glacier Tongue (TGT), Thwaites Eastern Ice Shelf (TEIS), Pine Island Basin, and Thwaites Basin. The pathways from the ice shelf fronts to the grounding lines are shown for (b) Pine Island, (c) Thwaites, (d) Smith, and (e) Kohler glaciers. Each pathway shows the trajectories 1,000 randomly sampled particles. The percentages indicate the mean \pm one standard deviation of the contribution from each pathway to the total particles at the grounding line. Red contours indicate the 1,000 m isobath where particles are initialized.

DINH ET AL. 3 of 11



Geophysical Research Letters

10.1029/2024GL110078

(Thomas et al., 2015; Vecchioni et al., 2023). As in prior studies, we assume that this simplification has a minimal influence on the derived particle pathways.

The positions, temperature, and salinity of the particles are recorded daily. Due to short water columns in the cavity, we use a 5 min time step to minimize overshoots that advect particles into dry cells. We do not employ an un-beaching algorithm. Instead, particles that hit a dry cell are removed from the analysis. Post-advection analysis shows that particles that hit land account for 11.7%, 2.9%, and 19.9%, 9.8% of the particles released at Pine Island, Thwaites, Smith, and Kohler, respectively. Almost all (>99%) particle beaching occurs within the ice cavity.

2.3. Temperature of the Particles

The temperature of the particles are recorded on a daily basis. We only measure the temperature change of particles that cross the ASE without looping the data fields. The temperature change is compared against the temperature baseline from the Ice Sheet Model Intercomparison for CMIP6 (ISMIP6), created to provide a reference temperature to propagate anomalies from the edge of the continental shelf into ice shelf cavities (Jourdain et al., 2020). We use the latitude and longitude (but not depth) of the particles to sample the ISMIP6 temperature at 690 m depth, which is the approximate depth of sills blocking the intrusions of CDW in the ASE. We do not use the particle depths because the pycnocline in SOhi is higher than in observations (Dinh et al., 2024b). Particles that travel along an isopycnal in SOhi could be crossing the pycnocline in the ISMIP6 reconstruction, which would bias the inferred temperature changes.

3. Results

3.1. Transport From Ice Shelf Fronts to Grounding Lines

We trace the pathways of particles at the grounding lines back in time to when they first entered the ice shelves. We combine all daily releases and report the mean $\pm 1\sigma$, where σ is the standard deviation of the 50th percentile time needed for the particles to reach the grounding lines.

For Pine Island (Figure 1b), the particles enter the cavity at the southern end of the ice front and travel counter-clockwise along the southern wall until reaching a sill at 700-m depth. The flow is deflected clockwise by the seafloor ridge before reaching the grounding line as in Dutrieux et al. (2014). On average, the particles take 55 ± 14 days to reach the grounding line.

For Thwaites (Figure 1c), we identify four pathways from the ice shelf front to the grounding line. The first three are the troughs labeled as T1, T2, and T3 discussed in Wåhlin et al. (2021) that connect the Thwaites basin to the northern edge of the Thwaites Glacier Tongue (TGT). T1 (Figure 1c, purple) transports $2 \pm 1\%$ of the particles in 72 ± 31 days. T2 (Figure 1c, red) transports $8 \pm 4\%$ in 60 ± 27 days. T3 (Figure 1c, blue) transports $3 \pm 2\%$ in 63 ± 44 days. The fourth pathway, T4 (Figure 1c, black), is through the Thwaites Eastern Ice Shelf (TEIS). We find that T4 transports the majority $(85 \pm 7\%)$ of the particles in 66 ± 13 days. A remaining $2 \pm 1\%$ is trapped in sub-shelf circulation for the entire 3 year duration. The inflow from these four pathways joins together and flows toward the grounding line within a single clockwise sub-shelf current. 55% of the particles travel directly to the grounding line while 45% get is re-circulated one or more times by the sub-shelf current (Figure S4 in Supporting Information S1).

For Smith (Figure 1d) and Kohler (Figure 1e) glaciers, the majority $(98 \pm 1\% \text{ and } 99 \pm 1\%, \text{ respectively})$ of particles enter through the Dotson Ice Shelf, flowing southward along the eastern wall before hitting a sill between the Crosson and Dotson ice shelves at ~775 m depth. Particles that travel past the sill flow along a deep trough to the grounding line of Smith in 59 ± 10 days. Particles that do not cross the sill meander eastward toward the grounding line of Kohler in 116 ± 15 days. Particles entering from the Crosson Ice Shelf have a negligible contribution of only $2 \pm 1\%$ in 160 ± 47 days for Smith and $1 \pm 1\%$ in 223 ± 70 days for Kohler.

3.2. Sources of CDW at the Grounding Lines

We trace particles back in time to identify where they first enter the ASE (i.e., sources). Particles enter the ASE either from off-shelf sources via submarine troughs or from east-shelf sources via the Antarctic Coastal Current (AACC). Probability distribution of the longitudes where off-shelf particles cross the shelf-break are provided in the supplementary (Figure S6 in Supporting Information S1). Particles entering from the west of ASE constitute

DINH ET AL. 4 of 11

com/doi/10.1029/2024GL110078 by Matthew R. Mazloff - University Of California , Wiley Online Library on [23/12/2024]. See the Terms and Conditions (https://online

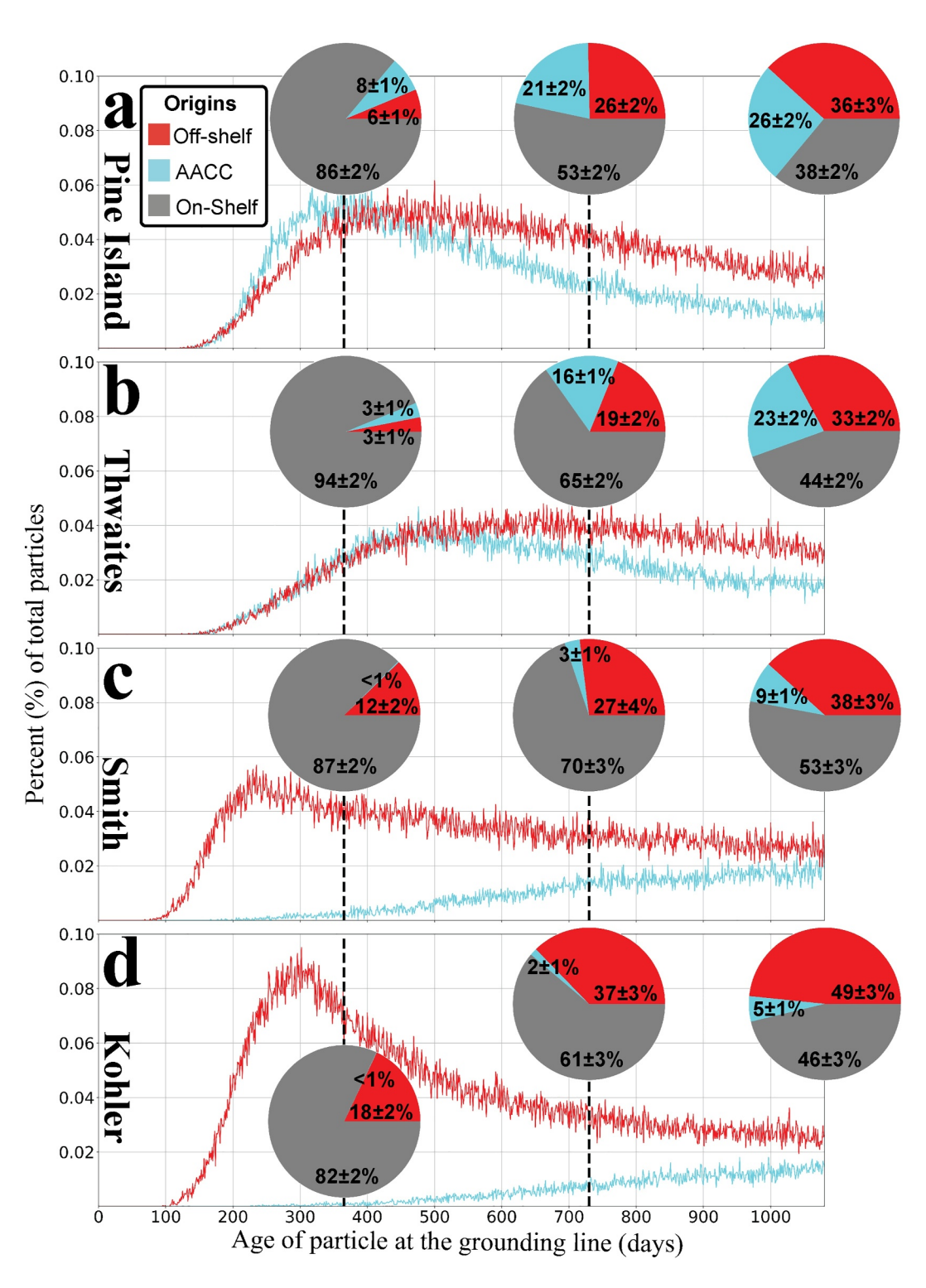


Figure 2. Age distribution of particles from when they enter the ASE until they reach the grounding lines of (a) Pine Island, (b) Thwaites, (c) Smith, and (d) Kohler glaciers. The mean \pm one standard deviation of water originating from off-shelf (red), east-shelf transported by the AACC (cyan), and within ASE (gray) after 1, 2, and 3 years is summarized in the pie charts.

less than 0.001% of the total. We find that 6%-18% of the particles originate from outside of the ASE in the previous year (Figures 2a-2d) and half (47%-62%) in the previous 3 years. For Pine Island and Thwaites, the AACC contributes equally to the amount of particles reaching the grounding lines as off-shelf sources. Pine Island

DINH ET AL. 5 of 11

wiley.com/doi/10.1029/2024GL110078 by Matthew R. Mazloff - University Of California , Wiley Online Library on [23/12/2024]. See the Terms and Conditions (https://online.com/doi/10.1029/2024GL110078 by Matthew R. Mazloff - University Of California , Wiley Online Library on [23/12/2024]. See the Terms and Conditions (https://online.com/doi/10.1029/2024GL110078 by Matthew R. Mazloff - University Of California , Wiley Online Library on [23/12/2024]. See the Terms and Conditions (https://online.com/doi/10.1029/2024GL110078 by Matthew R. Mazloff - University Of California , Wiley Online Library on [23/12/2024]. See the Terms and Conditions (https://online.com/doi/10.1029/2024GL110078 by Matthew R. Mazloff - University Of California , Wiley Online Library on [23/12/2024]. See the Terms and Conditions (https://online.com/doi/10.1029/2024GL110078 by Matthew R. Mazloff - University Of California , Wiley Online Library on [23/12/2024]. See the Terms and Conditions (https://online.com/doi/10.1029/2024GL110078 by Matthew R. Mazloff - University Of California , Wiley Online Library on [23/12/2024]. See the Terms and Conditions (https://online.com/doi/10.1029/2024GL110078 by Matthew R. Mazloff - University Online Library on [23/12/2024]. See the Terms and Conditions (https://online.com/doi/10.1029/2024GL110078 by Matthew R. Mazloff - University Online Library on [23/12/2024]. See the Terms of the Condition of

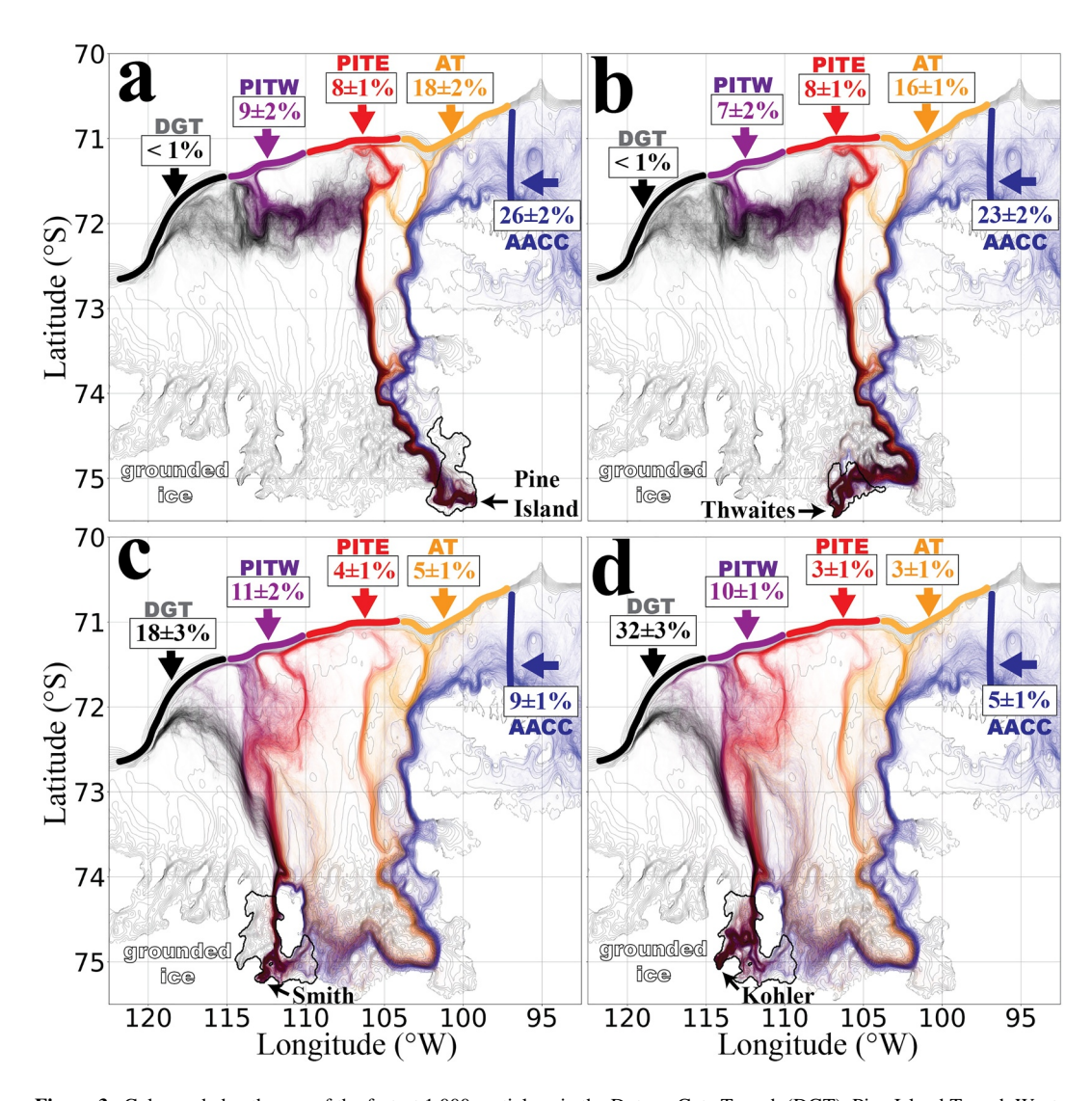


Figure 3. Color-coded pathways of the fastest 1,000 particles via the Dotson-Getz Trough (DGT), Pine Island Trough West (PITW), Pine Island Trough East (PITE), Abbot Trough (AT), and east-shelf transported by AACC to the grounding lines of (a) Pine Island, (b) Thwaites, (c) Smith, and (d) Kohler. The mean \pm one standard deviation is indicated as a percentage of the particles.

has $36 \pm 3\%$ from off-shelf versus $26 \pm 2\%$ from AACC (Figure 2a). For Thwaites, $33 \pm 2\%$ are off-shelf versus $23 \pm 2\%$ from AACC (Figure 2b). For Smith (Figure 2c) and Kohler (Figure 2d) $38 \pm 3\%$ and $49 \pm 3\%$ are from off-shelf, versus $9 \pm 1\%$ and 5 ± 1 from AACC, respectively.

The AACC flows east to west and transports modified CDW from the Bellingshausen Sea (BS) into the ASE along the Antarctic coastline. Inside the ASE, the AACC follows the coastline southward toward Pine Island and Thwaites (Figure 3, blue). Past Thwaites, the pathway becomes more poorly defined. A tiny fraction reaches Smith and Kohler glaciers through Crosson Ice Shelf. The majority meanders northward and enters the cavity of Dotson Ice Shelf.

Off-shelf waters reaching Pine Island (Figure 3a) and Thwaites (Figure 3b) glaciers via GDT and PITW travel eastward on the shelf before joining the southbound flow along PITE at 106° W. Particles entering from AT split into two distinct pathways: some particles follow the AACC, while the rest of them flow clockwise around the deepest part of the trough before joining PITE. Over 3 years, the fraction of particles coming from PITW and PITE is the same. Pine Island has $9 \pm 2\%$ from PITW and $8 \pm 1\%$ from PITE versus $7 \pm 2\%$ and $8 \pm 1\%$ for

DINH ET AL. 6 of 11

Thwaites. Contributions from the GDT are negligible with less than 1% for each glacier. AT is responsible for the largest amount of off-shelf particles with $18 \pm 2\%$ and $16 \pm 1\%$ for Pine Island and Thwaites, respectively.

For Smith (Figure 3c) and Kohler (Figure 3d), the DGT is the main source of off-shelf particles with $18\pm3\%$ and $32\pm3\%$ respectively. The second largest contributor is PITW with 10%-11% after 3 years. Particles that enter PITW, instead of turning eastward, continue south and cut through a region where the bed is 450 m deep. PITE and AT each contribute between 3% and 5% of the particles. The main pathway from PITE and AT to Smith and Kohler is southbound toward Pine Island and merging with the AACC. Some particles cross the 700 m isobath boundary at PITE, but continue westward along a shallower isobath on the shelf until PITW where they turn southward toward Smith and Kohler.

Optimum multiparameter (OMP) analysis (Frants et al., 2013) was conducted using temperature and salinity sampled by the particles to quantify contributions from Upper CDW (UCDW; 1.9 °C, 34.60 psμ), Lower CDW (LCDW; 1.3 °C, 34.75 psu), Winter Water (WW; -1.8 °C, 34.3 psu), and Antarctic Surface Water (AASW; -1.9 °C, 33 psu) (Figure S5 in Supporting Information S1). We base the definitions of water masses on (Biddle et al., 2017) and make slight adjustments according to the temperature and salinity in SOhi (Figure S2 in Supporting Information S1). Our results show that off-shelf particles are 80+% LCDW and UCDW, and AACC particles are 60+% LCDW and UCDW. For off-shelf particles, the percentages of CDWs are consistent over most of the run, and decrease as they enter the ice cavities and approach the grounding lines. For particles traveling along the AACC, CDWs fraction increases to a maximum around 3–6 months prior to reaching the grounding lines, and then decreases in a similar fashion to the off-shelf particles.

3.3. Cooling During Transport to the Grounding Lines

For Pine Island and Thwaites, the fastest particles to the grounding lines are east-shelf AACC sources and off-shelf sources via PITE and AT. Overall, off-shelf particles reaching Pine Island (Figure 4a) cool by 0.6° C, including 0.2° C on the continental shelf and 0.4° C in the cavity. Particles reaching Thwaites (Figure 4b) cool by 0.8° C, including 0.3° C on the continental shelf and 0.5° C in the cavity. In contrast, the colder east-shelf particles warm by 0.6 to 0.8° C as they travel through the continental shelf and mix with warm CDW. For Smith and Kohler, the fastest particles are off-shelf particles traveling through GDT or PITW. The temperature for Smith (Figure 4c) decreases by 1° C, with 0.6° C on the continental shelf and 0.4° C in the cavity. For Kohler (Figure 4d), the cooling is 0.8° C, with 0.6° C on the continental shelf and 0.2° C in the cavity.

The ISMIP6 temperature reconstruction shows a net cooling from the shelf-break to the grounding lines (Figure 4, black). We compare the cooling at 690 m since this is the depth of the sills blocking the intrusion of CDW in this region. For Pine Island and Thwaites, the cooling is 0.5°C from the shelf-break to the ice shelf fronts, with no additional cooling in the ice shelf cavities. For Smith and Kohler, there is a 1.4-1.5°C cooling from the shelf-break to the ice shelf front and a 0.6-0.9°C warming in the cavities, for a net cooling of 0.6-0.8°C.

4. Discussion

Prior work has focused on understanding the processes bringing warm CDW onto the ASE (Assmann et al., 2013; Dinniman & Klinck, 2004; Wåhlin et al., 2012). Here, we quantify the timescales, cooling, and contribution of various pathways to the grounding lines. We find that the median age of particles at grounding lines is 3 years from the time when they entered the ASE. Half (38%–53%) of the water at the grounding line spends over 3 years on the continental shelf and ice shelf cavities. Annual and inter-annual changes in continental shelf dynamics may therefore have a stronger impact on ocean thermal forcing at the grounding lines than anomalies in off-shelf sources. The continental shelf acts as a buffer zone between the glaciers and off-shelf CDW anomalies. Offshelf changes in CDW will impact the glaciers mostly over multiple years. We also find that the AACC plays a major role in contributing to water properties in the cavities. Previous work revealed a connectivity between the West Antarctic Peninsula (WAP) and the ASE through the Bellingshausen Sea (BS) (Dawson et al., 2023; Flexas et al., 2022; Hyogo et al., 2024; Schubert et al., 2021). Park et al. (2024) suggested that the AACC plays a role in controlling the thermocline depth in the ASE, which in turn controls the CDW inflow into the cavities. Here, we document that an equal amount of east-shelf water reaches the grounding lines of Pine Island and Thwaites glaciers as off-shelf sources in 3 years. AACC water is colder than off-shelf water, hence contributes a cooling of CDW before it reaches the glacier grounding lines. Changes in the BS and WAP will therefore impact the basal melting regime of Pine Island, Thwaites, as much as changes in off-shelf CDW sources. The equal importance of

DINH ET AL. 7 of 11

19448070, 2024, 19, Downloaded from https://gutpubs.nimielibrary.wiley.com/doi/10.1099/2024G11.10078 by Matthew R. Mazloff - University Of California, Wiley Online Library on [23/12/2024]. See the Terms and Conditions (https://onlinelibrary.wiley.com/doi/10.1099/2024G1.10078 by Matthew R. Mazloff - University Of California, Wiley Online Library on [23/12/2024]. See the Terms and Conditions (https://onlinelibrary.wiley.com/doi/10.1099/2024G1.10078 by Matthew R. Mazloff - University Of California, Wiley Online Library on [23/12/2024]. See the Terms and Conditions (https://onlinelibrary.wiley.com/doi/10.1099/2024G1.10078 by Matthew R. Mazloff - University Of California, Wiley Online Library on [23/12/2024]. See the Terms and Conditions (https://onlinelibrary.wiley.com/doi/10.1099/2024G1.10078 by Matthew R. Mazloff - University Of California, Wiley Online Library on [23/12/2024]. See the Terms and Conditions (https://onlinelibrary.wiley.com/doi/10.1099/2024G1.10078 by Matthew R. Mazloff - University Of California, Wiley Online Library on [23/12/2024]. See the Terms and Conditions (https://onlinelibrary.wiley.com/doi/10.1099/2024G1.10078 by Matthew R. Mazloff - University Of California, Wiley Online Library on [23/12/2024]. See the Terms and Conditions (https://onlinelibrary.wiley.com/doi/10.1099/2024G1.10078 by Matthew R. Mazloff - University Of California, Wiley Online Library on [23/12/2024]. See the Terms and Conditions (https://onlinelibrary.wiley.com/doi/10.1099/2024G1.10078 by Matthew R. Mazloff - University Of California, Wiley Online Library on [23/12/2024]. See the Terms and Conditions (https://onlinelibrary.wiley.com/doi/10.1099/2024G1.10078 by Matthew R. Mazloff - University Of California, Wiley Online Library on [23/12/2024]. See the Terms and Conditions (https://onlinelibrary.wiley.com/doi/10.1099/2024G1.10078 by Matthew R. Mazloff - University Of California, Wiley Online Library on [23/12/2024]. See the Terms and Conditions (https://onlinelibrary.wiley.com/doi/10.1099/2024G1.10078 by Matthew R. Mazlof

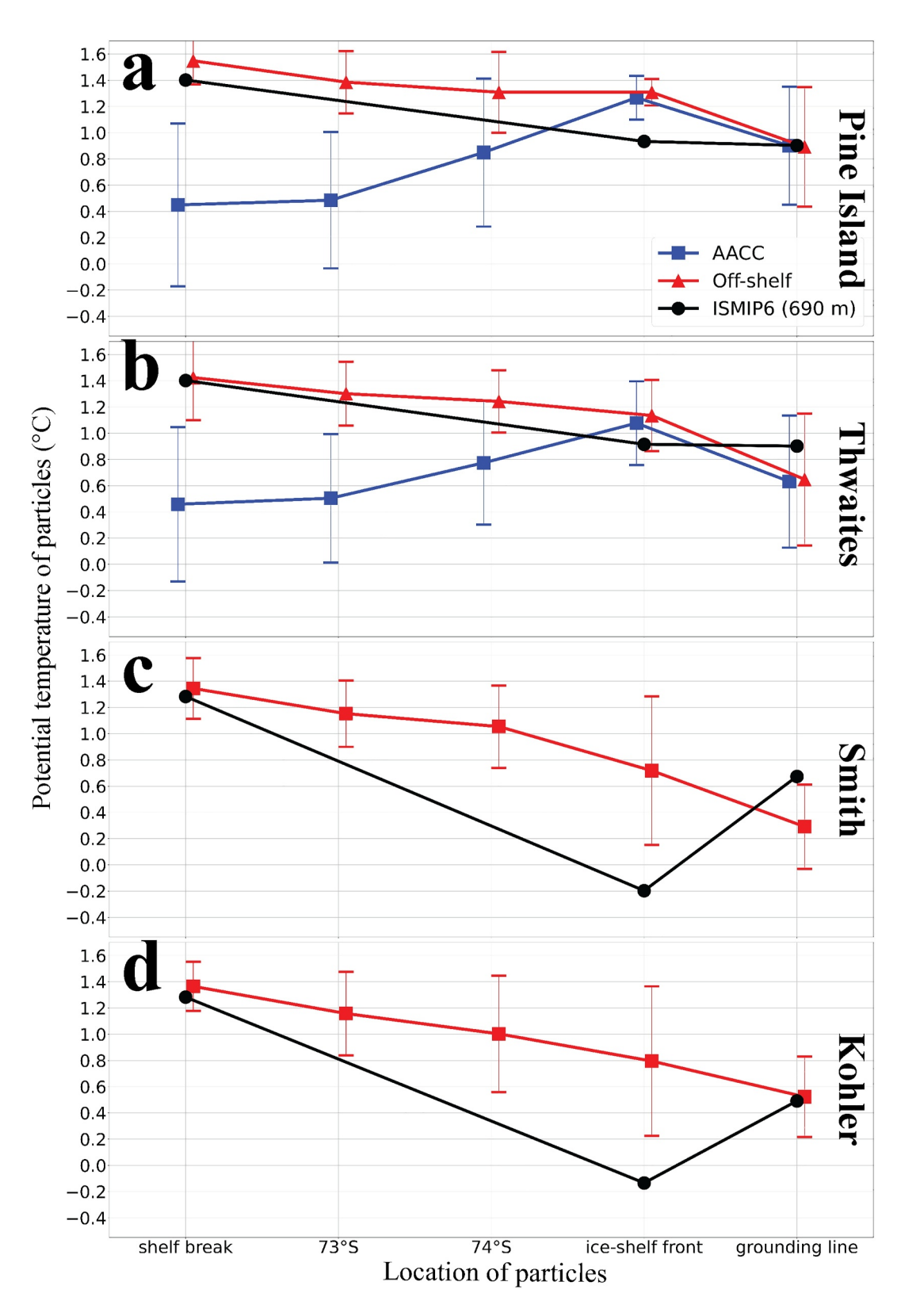


Figure 4. Temperature (mean \pm one standard deviation) change of the fastest particles (<1 year) propagating from off-shelf sources (red) and AACC (blue) from the shelf break (or east-shelf boundary shown in Figure 1 for AACC) to the grounding lines of (a) Pine Island, (b) Thwaites, (c) Smith, and (d) Kohler glaciers versus temperature changes from the ISMIP6 baseline temperature reconstruction at 690 m depth (black). Note that the temperature of particles at the grounding lines is recorded one day prior to particles actually arriving at the grounding line.

DINH ET AL. 8 of 11

AACC and off-shelf sources in modulating ocean thermal forcing is relevant for modeling projections. The validity of this result in other years and over the longer term needs to be further evaluated.

Previous work from Nakayama et al. (2019) indicated a pathway to Thwaites that splits from the southward flow to Pine Island at 74.2°S, entering TGT from the Thwaites Basin through T2. We see some particles following this pathway in our analysis (Figure S7 in Supporting Information S1), but the majority of the particles in our model enter Thwaites through the TEIS (T4). We attribute this discrepancy to the fact that particles in Nakayama et al. (2019) represent only CDW found in deep troughs leading to Thwaites. In contrast, the particles in our study represent all water parcels that reach the grounding line, that is, a fraction of them are shallower and cooler. In addition, we find that only 55% of the particles flow directly to the grounding line past the ice shelf fronts. About 45% are trapped in a sub-shelf current and recirculate one or more times inside the cavity (Figure S4 in Supporting Information S1). This sub-shelf current increases mixing and results in colder water of non-CDW origin at the grounding line. This pathway explains why the model cooling of 0.5°C from the ice shelf front to the grounding line is slightly larger for Thwaites than for Pine Island (0.4°C), Smith (0.4°C), and Kohler (0.2°C).

Another important finding of this study is that the main source of warm CDW to the grounding line of Smith is from DGT via the Dotson Ice Shelf whereas the Crosson Ice Shelf plays a negligible role. Smith and Kohler share the same ocean thermal ocean forcing, separate from the CDW sources feeding Pine Island and Thwaites glaciers. The longer traveling distance to Smith grounding line explains the higher degree of water cooling compared to Kohler.

The ISMIP6 baseline uses a mathematical extrapolation in the ice shelf cavities and hence indicates no effective cooling (Figure 4, Figure S8 in Supporting Information S1) and even introduces a 0.6-0.9°C warming for Smith and Kohler. In contrast, we find that 25%–66% of the cooling between the shelf-break and the grounding lines occurs within the ice cavities. The ISMIP6 baseline therefore overestimates ocean thermal forcing at the grounding lines, which in turn overestimates the ice shelf melt rate. The temperature-melt relationships derived from SOhi may inform the ISMIP6 baseline and estimates of ocean heat transfer inside the cavities, but the sensitivity of these relationships to model configuration and interannual variability deserves further studies.

Field observations from Wåhlin et al. (2021) showed that T2 and T3, connecting with the TGT, are 100–300 m deeper than known previously. The authors estimate that T3 (Figure 2b) transports 0.8 TW of heat into the cavity and impacts the melt regime of the entire ice shelf (Wåhlin et al., 2021). In SOhi and Nakayama et al. (2019), water flow through T3 is more restricted by a bathymetric high. While we expect that updating the bathymetry with deeper troughs at T2 and T3 will slightly increase their contribution to TGT, it is unlikely that this adjustment will change the dominant pathway through TEIS that controls $85 \pm 7\%$ of the particles in SOhi. Recent work by St-Laurent et al. (2024) indeed shows that TEIS accounts for 60%–76% of the heat flux into the cavity. We conclude that T4 through the cavity of TEIS is a main source of ocean thermal forcing for TGT. Changes in the TEIS, for instance a collapse of the ice shelf, could affect CDW flow to TGT and in turn affect thermal forcing at the GL of the most active part of Thwaites, that is, TGT. As a result, we recommend more detailed bathymetric survey of the cavity of TEIS to improve the modeling of ice-ocean interaction in this region.

A limitation of our study is that only a single year of SOhi output is used in the analysis. The particles have to be advected with a looping velocity field, which may introduce an unrealistic discontinuity adding to the uncertainty of our results. In addition, as reported by Dinh et al. (2024a), the thermocline in SOhi is about 200 m too high in the ASE. A shallower thermocline may influence local processes and circulations and alter how particles are transported to the grounding lines. The Amundsen Sea Embayment is also a region known to experience strong inter-annual variability on the continental shelf (Dutrieux et al., 2014). Previous works have shown that year-to-year changes in icescape alter the regional circulation, strengths of pathways, and cooling of CDW into the cavity (Cougnon et al., 2017; St-Laurent et al., 2024). The results of our study are only applicable to the simulated years of 2005 and 2006. The robustness of our results needs to be further tested with additional observations and longer model runs. In the meantime, the study presents a first assessment of CDW transport to the grounding lines of glaciers in a critical sector of West Antarctica.

5. Conclusions

We use Lagrangian particles advected backwards from the grounding lines of Pine Island, Thwaites, Smith, and Kohler glaciers, to identify their sources, cooling, and pathways across the ASE. About half (38%–53%) of the

DINH ET AL. 9 of 11

Acknowledgments

Research Council.

This work was performed at the University

of California Irvine and San Diego and at

Caltech's Jet Propulsion Laboratory under

Analysis, and Prediction (MAP) Program.

80NSSC22K0387, and NSF Grants OCE-1924388, OPP-2149501, OPP-1936222,

MRM also acknowledges support from

and OPP-2319829. This study contains

data supplied by Natural Environment

NASA Grants 80NSSC24K0243 and

Award 80NSSC20K1076 from the

Administration (NASA) Modelling,

National Aeronautics and Space

water reaching grounding lines is on-shelf water that resided three or more years in ASE, hence buffering anomalies from off-shelf CDW sources. We detect a major contribution from the AACC toward the grounding lines of Pine Island and Thwaites, suggesting a direct connection between the Bellingshausen Sea and the ASE in controlling the evolution of ice shelf melt rates. Conversely, the ocean thermal forcing of Kohler and Smith is predominately and independently determined by the inflow of CDW through the DGT. Finally, we find that 25%–66% of the cooling during transport of CDW occurs in the ice shelf cavities, a factor that is not included in ISMIP6, which will reduce ocean thermal forcing on the glacier grounding lines.

Data Availability Statement

ISMIP6 baseline reconstruction tempterature are available via Ghub at https://theghub.org/dataset-listing. Particle trajectories for four glaciers and the SOhi mean temperature/salinity used for validation are archived on Dryad (Dinh et al., 2024a). Codes used to process data and generate the figures is archived on Zenodo (Dinh, 2024).

References

- Adusumilli, S., Fricker, H. A., Medley, B., Padman, L., & Siegfried, M. R. (2020). Interannual variations in meltwater input to the Southern Ocean from Antarctic ice shelves. *Nature Geoscience*, 13(9), 616–620. https://doi.org/10.1038/s41561-020-0616-z
- Assmann, K. M., Jenkins, A., Shoosmith, D. R., Walker, D. P., Jacobs, S. S., & Nicholls, K. W. (2013). Variability of circumpolar deep water transport onto the Amundsen Sea continental shelf through a shelf break trough. *Journal of Geophysical Research: Oceans*, 118(12), 6603–6620. https://doi.org/10.1002/2013JC008871
- Biddle, L. C., Heywood, K. J., Kaiser, J., & Jenkins, A. (2017). Glacial meltwater identification in the Amundsen Sea. *Journal of Physical Oceanography*, 47(4), 933–954. https://doi.org/10.1175/JPO-D-16-0221.1
- Cougnon, E. A., Galton-Fenzi, B. K., Rintoul, S. R., Legrésy, B., Williams, G. D., Fraser, A. D., & Hunter, J. R. (2017). Regional changes in icescape impact shelf circulation and basal melting. *Geophysical Research Letters*, 44(22), 11519–11527. https://doi.org/10.1002/2017GI 074943
- Dawson, H. R. S., Morrison, A. K., England, M. H., & Tamsitt, V. (2023). Pathways and timescales of connectivity around the antarctic continental shelf. *Journal of Geophysical Research: Oceans*, 128(2), e2022JC018962. https://doi.org/10.1029/2022JC018962
- Delandmeter, P., & Van Sebille, E. (2019). The Parcels v2.0 Lagrangian framework: New field interpolation schemes. *Geoscientific Model Development*, 12(8), 3571–3584. https://doi.org/10.5194/gmd-12-3571-2019
- Dinh, A. (2024). ah-dinh/Dinh_2024b: Initial_2024_04_30. Zenodo. [Software]. https://doi.org/10.5281/zenodo.11095757
- Dinh, A., Rignot, E., Mazloff, M., & Fenty, I. (2024a). Modeling ocean heat transport to the grounding lines of pine island, thwaites, smith, and kohler glaciers, west Antarctica. DRYAD. [Dataset]. https://doi.org/10.5061/dryad.8sf7m0cwt
- Dinh, A., Rignot, E., Mazloff, M., & Fenty, I. (2024b). Southern ocean high-resolution (SOhi) modeling along the antarctic ice sheet periphery. Geophysical Research Letters, 51(3), e2023GL106377. https://doi.org/10.1029/2023GL106377
- Dinniman, M. S., & Klinck, J. M. (2004). A model study of circulation and cross-shelf exchange on the west Antarctic Peninsula continental shelf. Deep-Sea Res. II: Top. Stud. Oceanogr., 51(17), 2003–2022. https://doi.org/10.1016/j.dsr2.2004.07.030
- Dinniman, M. S., Klinck, J. M., & Hofmann, E. E. (2012). Sensitivity of circumpolar deep water transport and ice shelf basal melt along the West antarctic peninsula to changes in the winds. *Journal of Climate*, 25(14), 4799–4816. https://doi.org/10.1175/JCLI-D-11-00307.1
- Dotto, T. S., Naveira Garabato, A. C., Bacon, S., Holland, P. R., Kimura, S., Firing, Y. L., et al. (2019). Wind-Driven processes controlling oceanic heat delivery to the Amundsen Sea, Antarctica. *Journal of Physical Oceanography*, 49(11), 2829–2849. https://doi.org/10.1175/JPO-D-19-0064.1
- Dutrieux, P., Rydt, J. D., Jenkins, A., Holland, P. R., Ha, H. K., Lee, S. H., et al. (2014). Strong sensitivity of pine island ice-shelf melting to climatic variability. *Science*, 343(6167), 174–178. https://doi.org/10.1126/science.1244341
- ECCO Consortium, Fukumori, I., Wang, O., Fenty, I., Forget, G., Heimbach, P., & Ponte, R. M. (2021). Synopsis of the ECCO central production global ocean and sea-ice state estimate. Version 4 Release 4 (Tech. Rep.). https://doi.org/10.5281/ZENODO.4533349
- Flexas, M. M., Thompson, A. F., Schodlok, M. P., Zhang, H., & Speer, K. (2022). Antarctic peninsula warming triggers enhanced basal melt rates throughout west Antarctica. *Science Advances*, 8(32), eabj9134. https://doi.org/10.1126/sciadv.abj9134
- Frants, M., Gille, S. T., Hewes, C. D., Holm-Hansen, O., Kahru, M., Lombrozo, A., et al. (2013). Optimal multiparameter analysis of source water distributions in the Southern Drake Passage. *Deep-Sea Res. II*, 90, 31–42. https://doi.org/10.1016/j.dsr2.2012.06.002
- GEBCO Bathymetric Compilation Group. (2020). The GEBCO_2020 Grid A continuous terrain model of the global oceans and land. British Oceanographic Data Centre. [Dataset]. https://doi.org/10.5285/A29C5465-B138-234D-E053-6C86ABC040B9
- Gudmundsson, G. H., Paolo, F. S., Adusumilli, S., & Fricker, H. A. (2019). Instantaneous Antarctic ice sheet mass loss driven by thinning ice shelves. Geophysical Research Letters, 46(23), 13903–13909. https://doi.org/10.1029/2019GL085027
- Holland, P. R., O'Connor, G. K., Bracegirdle, T. J., Dutrieux, P., Naughten, K. A., Steig, E. J., et al. (2022). Anthropogenic and internal drivers of wind changes over the Amundsen Sea, West Antarctica, during the 20th and 21st centuries. The Cryosphere, 16(12), 5085–5105. https://doi.org/10.5194/tc-16-5085-2022
- Hyogo, S., Nakayama, Y., & Mensah, V. (2024). Modeling Ocean circulation and ice shelf melt in the Bellingshausen Sea. *Journal of Geophysical Research: Oceans*, 129(3), e2022JC019275. https://doi.org/10.1029/2022JC019275
- Joughin, I., Smith, B. E., & Medley, B. (2014). Marine ice sheet collapse potentially under way for the Thwaites Glacier basin, west Antarctica. Science, 344(6185), 735–738. https://doi.org/10.1126/science.1249055
- Jourdain, N. C., Asay-Davis, X., Hattermann, T., Straneo, F., Seroussi, H., Little, C. M., & Nowicki, S. (2020). A protocol for calculating basal melt rates in the ismip6 antarctic ice sheet projections. *The Cryosphere*, 14(9), 3111–3134. https://doi.org/10.5194/tc-14-3111-2020
- Mazloff, M. R., Heimbach, P., & Wunsch, C. (2010). An eddy-permitting Southern Ocean State estimate. *Journal of Physical Oceanography*, 40(5), 880–899. https://doi.org/10.1175/2009JPO4236.1

DINH ET AL. 10 of 11

- Morlighem, M. (2019). MEaSUREs BedMachine Antarctica Version 1. NASA National Snow and Ice Data Center Distributed Active Archive Center. [Dataset]. https://doi.org/10.5067/C2GFER6PTOS4. Accessed: Jun 2020.
- Nakayama, Y., Manucharyan, G., Zhang, H., Dutrieux, P., Torres, H. S., Klein, P., et al. (2019). Pathways of ocean heat towards Pine Island and Thwaites grounding lines. *Scientific Reports*, 9(1), 16649. https://doi.org/10.1038/s41598-019-53190-6
- Nakayama, Y., Menemenlis, D., Zhang, H., Schodlok, M., & Rignot, E. (2018). Origin of circumpolar deep water intruding onto the amundsen and Bellingshausen Sea continental shelves. *Nature Communications*, 9(1), 3403. https://doi.org/10.1038/s41467-018-05813-1
- Naughten, K. A., Holland, P. R., Dutrieux, P., Kimura, S., Bett, D. T., & Jenkins, A. (2022). Simulated twentieth-century ocean warming in the amundsen sea, west Antarctica. Geophysical Research Letters, 49(5). https://doi.org/10.1029/2021GL094566
- Nowicki, S., & Seroussi, H. (2018). Projections of future sea level contributions from the Greenland and antarctic ice sheets: Challenges beyond dynamical ice sheet modeling. *Oceanography*, 31(2), 109–117. https://doi.org/10.5670/oceanog.2018.216
- Park, T., Nakayama, Y., & Nam, S. (2024). Amundsen Sea circulation controls bottom upwelling and Antarctic Pine Island and Thwaites ice shelf melting. *Nature Communications*, 15(1), 2946. https://doi.org/10.1038/s41467-024-47084-z
- Pritchard, H. D., Ligtenberg, S. R. M., Fricker, H. A., Vaughan, D. G., Van Den Broeke, M. R., & Padman, L. (2012). Antarctic ice-sheet loss driven by basal melting of ice shelves. *Nature*, 484(7395), 502–505. https://doi.org/10.1038/nature10968
- Rignot, E., Bamber, J. L., Van Den Broeke, M. R., Davis, C., Li, Y., Van De Berg, W. J., & Van Meijgaard, E. (2008). Recent Antarctic ice mass loss from radar interferometry and regional climate modelling. *Nature Geoscience*, 1(2), 106–110. https://doi.org/10.1038/ngeo102
- Rignot, E., Jacobs, S., Mouginot, J., & Scheuchl, B. (2013). Ice-shelf melting around Antarctica. Science, 341(6143), 266–270. https://doi.org/10.
- Rignot, E., Mouginot, J., Morlighem, M., Seroussi, H., & Scheuchl, B. (2014). Widespread, rapid grounding line retreat of pine island, thwaites, smith, and kohler glaciers, west Antarctica, from 1992 to 2011. *Geophysical Research Letters*, 41(10), 3502–3509. https://doi.org/10.1002/
- Rignot, E., Mouginot, J., Scheuchl, B., Van Den Broeke, M., Van Wessem, M. J., & Morlighem, M. (2019). Four decades of antarctic ice sheet mass balance from 1979–2017. *Proceedings of the National Academy of Sciences*, 116(4), 1095–1103. https://doi.org/10.1073/pnas.1812883116
- Schubert, R., Thompson, A. F., Speer, K., Schulze Chretien, L., & Bebieva, Y. (2021). The antarctic coastal current in the bellingshausen sea. *The Cryosphere*, 15(9), 4179–4199. https://doi.org/10.5194/tc-15-4179-2021
- Stewart, A. L., & Thompson, A. F. (2015). Eddy-mediated transport of warm circumpolar deep water across the antarctic shelf break. *Geophysical Research Letters*, 42(2), 432–440. https://doi.org/10.1002/2014GL062281
- St-Laurent, P., Klinck, J. M., & Dinniman, M. S. (2013). On the role of coastal troughs in the circulation of warm circumpolar deep water on antarctic shelves. *Journal of Physical Oceanography*, 43(1), 51–64. https://doi.org/10.1175/JPO-D-11-0237.1
- St-Laurent, P., Stammerjohn, S. E., & Maksym, T. (2024). Response of onshore oceanic heat supply to yearly changes in the amundsen sea icescape (Antarctica). *Journal of Geophysical Research: Oceans*, 129(4), e2023JC020467. https://doi.org/10.1029/2023JC020467
- Thomas, M. D., Tréguier, A.-M., Blanke, B., Deshayes, J., & Voldoire, A. (2015). A Lagrangian method to isolate the impacts of mixed layer subduction on the meridional overturning circulation in a numerical model. *Journal of Climate*, 28(19), 7503–7517. https://doi.org/10.1175/
- Thompson, A. F., Stewart, A. L., Spence, P., & Heywood, K. J. (2018). The antarctic slope current in a changing climate. *Reviews of Geophysics*, 56(4), 741–770. https://doi.org/10.1029/2018RG000624
- Vecchioni, G., Cessi, P., Pinardi, N., Rousselet, L., & Trotta, F. (2023). A Lagrangian estimate of the mediterranean outflow's origin. *Geophysical Research Letters*, 50(14), e2023GL103699. https://doi.org/10.1029/2023GL103699
- Velicogna, I., Sutterley, T. C., & Van Den Broeke, M. R. (2014). Regional acceleration in ice mass loss from Greenland and Antarctica using GRACE time-variable gravity data. *Geophysical Research Letters*, 41(22), 8130–8137. https://doi.org/10.1002/2014GL061052
- Wåhlin, A. K., Graham, A. G. C., Hogan, K. A., Queste, B. Y., Boehme, L., Larter, R. D., et al. (2021). Pathways and modification of warm water flowing beneath thwaites ice shelf, west Antarctica. Science Advances, 7(15), eabd7254, https://doi.org/10.1126/sciady.abd7254
- Wåhlin, A. K., Muench, R. D., Arneborg, L., Björk, G., Ha, H. K., Lee, S. H., & Alsén, H. (2012). Some implications of ekman layer dynamics for cross-shelf exchange in the Amundsen Sea. *Journal of Physical Oceanography*, 42(9), 1461–1474. https://doi.org/10.1175/JPO-D-11-041.1
- Weertman, J. (1974). Stability of the junction of an ice sheet and an ice shelf. *Journal of Glaciology*, 13(67), 3–11. https://doi.org/10.1017/s0022143000023327

DINH ET AL. 11 of 11